Published in final edited form as:
DNA Repair (Amst). 2010 June 4; 9(6): 643–652. doi:10.1016/j.dnarep.2010.02.014.

RPA PHYSICALLY INTERACTS WITH THE HUMAN DNA GLYCOSYLASE NEIL1 TO REGULATE EXCISION OF OXIDATIVE DNA BASE DAMAGE IN PRIMER-TEMPLATE STRUCTURES

Corey A. Theriot[a], **Muralidhar L. Hegde**[a], **Tapas K. Hazra**[a,b], and **Sankar Mitra**[a]

Corey A. Theriot: corey.theriot@nasa.gov; Muralidhar L. Hegde: mlhegde@utmb.edu; Tapas K. Hazra: tkhazra@utmb.edu; Sankar Mitra: samitra@utmb.edu

[a]Department of Biochemistry and Molecular Biology, University of Texas Medical Branch, 301 University Boulevard, Galveston, TX 77555.

[b]Department of Internal Medicine, University of Texas Medical Branch, 301 University Boulevard, Galveston, TX 77555.

Abstract

The human DNA glycosylase NEIL1, activated during the S-phase, has been shown to excise oxidized base lesions in single-strand DNA substrates. Furthermore, our previous work demonstrating functional interaction of NEIL1 with PCNA and flap endonuclease 1 (FEN1) suggested its involvement in replication-associated repair. Here we show interaction of NEIL1 with replication protein A (RPA), the heterotrimeric single-strand DNA binding protein that is essential for replication and other DNA transactions. The NEIL1 immunocomplex isolated from human cells contains RPA, and its abundance in the complex increases after exposure to oxidative stress. NEIL1 directly interacts with the large subunit of RPA (K_d ~20 nM) via the common interacting interface (residues 312–349) in NEIL1's disordered C-terminal region. RPA inhibits the base excision activity of both wild type NEIL1 (389 residues) and its C-terminal deletion CΔ78 mutant (lacking the interaction domain) for repairing 5-hydroxyuracil (5-OHU) in a primer-template structure mimicking the DNA replication fork. This inhibition is reduced when the damage is located near the primer-template junction. Contrarily, RPA moderately stimulates wild-type NEIL1 but not the CΔ78 mutant when 5-OHU is located within the duplex region. While NEIL1 is inhibited by both RPA and *E. coli* single-strand DNA binding protein, only inhibition by RPA is relieved by PCNA. These results showing modulation of NEIL1's activity on single-stranded DNA substrate by RPA and PCNA support NEIL1's involvement in repairing the replicating genome.

Keywords

base excision repair; replicating-associated repair; protein-protein interaction; DNA glycosylase; NEIL1; RPA

Address correspondence to: Sankar Mitra, University of Texas Medical Branch, Department of Biochemistry and Molecular Biology, 6.136 Medical Research Building, Galveston, TX 77555-1079; Telephone: 409-772-1780/1788; Fax: 409-747-8608, samitra@utmb.edu.

1.1 Introduction

Reactive oxygen species (ROS) continuously produced as by-products of cellular respiration and metabolism of toxic compounds, and also generated after inflammation and exposure to ionizing radiation, comprise the most pervasive genotoxic agents [1–3]. ROS-induced DNA damage includes oxidatively modified bases (i.e., 8-oxoguanine, thymine glycol 5-hydroxyuracil, and formamidopyrimidines, etc.), abasic (apurinic/apyrimidinic; AP) sites and DNA strand breaks. Most of these lesions are potentially mutagenic and have been implicated in the etiology of various diseases including cancer, degenerative neurological disorders, arthritis, and also in aging and cellular toxicity [4–9]. These base damages are repaired primarily via the DNA base excision repair (BER) pathway, a highly conserved process that is initiated with excision of the lesion by a DNA glycosylase [10].

Four human DNA glycosylases with overlapping and broad substrate range, and belonging to two families named after the *E. coli* prototype enzymes, are primarily responsible for repairing several dozen oxidatively modified bases. All oxidized base-specific glycosylases possess intrinsic AP lyase activity and cleave the DNA strand at the AP site after base excision [11]. The human Nth family members OGG1 and NTH1 carry out β elimination to produce 3′ phosphodeoxyribose (3′ dRP) terminus at the strand break while the glycosylases in the Nei family possess β,δ-lyase activity to generate 3′ phosphate [12,13]. We and others have identified and characterized mammalian orthologs of the Nei family which we named NEILs [14–18]. The 3′dRP or 3′ phosphate blocking group generated by the Nth or Nei type glycosylases is removed in mammalian cells by AP endonuclease (APE1) or polynucleotide kinase (PNK) respectively to generate 3′ OH [19,20]. In the basic BER process, DNA polymerase β (Pol β) fills in the single nucleotide gap and in the final step, DNA ligase IIIα (Lig IIIα) seals the nick to restore genome integrity in the single nucleotide (SN) BER pathway [21,22]. Recent studies in our and other laboratories have shown that the BER pathway is more complex than observed in single-nucleotide repair (SN-BER), with cross-talk occurring between the core components of BER and DNA metabolic pathways including transcription and replication. Multiple repair sub-pathways are likely to be active *in vivo*. Dou *et al.*, demonstrated that NEIL1 and NEIL2 unlike OGG1 and NTH1 are able to excise oxidized base lesions from regions of single-stranded DNA suggesting a role for NEIL-initiated repair of oxidative DNA damage during replication and/or transcription [23].

Our early studies of NEIL1-initiated BER showed pairwise interaction of NEIL1 (and NEIL2) with downstream components of the SN-BER pathway including Pol β, Lig IIIα and XRCC1 suggesting formation of a repair complex in which NEIL1(and NEIL2) play a critical role in coordinating subsequent repair steps after base excision [20,48]. We have recently shown that NEIL1 also interacts with and is activated by several proteins which are involved in DNA replication or intermediate processing. Thus we observed physical and functional interaction of NEIL1 with Werner syndrome protein (WRN), a RecQ family DNA helicase whose deficiency is associated with early onset of aging and which may restore collapsed replication forks [24]. We also showed binary interaction of NEIL1 with proliferating cell nuclear antigen (PCNA), the sliding clamp responsible for DNA polymerase processivity, and flap endonuclease 1 (FEN1), an essential 5′ endo/exonuclease required for the removal of Okazaki fragments in the lagging strand during DNA replication [25,26]. All of these proteins stimulate NEIL1 activity with various substrate structures [24–26]. The replication factor C (RFC), that loads the PCNA clamp onto the primed DNA template, was also identified in the NEIL1 complex [25]. Furthermore, Lu's group, in collaboration with us, showed that NEIL1 stably interacts with and is stimulated by the Rad9-Rad1-Hus1 (9-1-1) complex, a damage-activated DNA sliding clamp that replaces PCNA upon p21 activation and replication arrest [27]. The discovery of functional interaction between NEIL1 and DNA replication-associated proteins, NEIL1's S-phase specific up-regulation and activity with single-stranded (ss) DNA substrate

prompted us to hypothesize that NEIL1 is involved in preferential repair of oxidative base damage in the replicating genome.

In order to test for physical association of various replication proteins with NEIL1, we carried out systematic Western analysis of the NEIL1 immunocomplex isolated from nuclear extracts of HeLa and HCT 116 cells. We identified replication protein A (RPA), the major ssDNA binding protein in eukaryotes initially discovered as an essential factor in SV40 DNA replication and later shown to be also essential for cellular DNA replication [28–30]. The heterotrimeric RPA is composed of three subunits namely, 70-kDa RPA1, 32-kDa RPA2, and 14-kDa RPA3 [31]. Although a recent study implicated another mammalian ssDNA binding protein in DNA transactions [32], RPA has been shown to be involved in a variety of DNA damage responses [33]. Native RPA possesses four DNA-binding domains (DBD), A–D, which independently bind to ssDNA with decreasing affinity from A to D. The domains (DBD-A, -B and -C) are present in RPAl while DBD-D is located in the RPA2 [34]. The DBDs initiate binding at the 5′ end of ssDNA starting with DBD-A and –B occluding 8–10 nucleotides [35, 36]. Then, via conformational change, DBD-C binds to cover a stretch of 12–23 nucleotides [37]. Finally, co-operative binding of all four DBDs results in a fully extended conformation of RPA covering a stretch of approximately 30 nucleotides [38,39]. These three distinct states of binding are believed to coexist and native RPA may undergo change between extended and compact conformations depending on the need to cover the ssDNA stretch [40].

RPA (~ 10^5 molecules/cell), one of the more abundant cellular proteins, interacts with a number of proteins in various DNA metabolic pathways including DNA replication, repair, recombination and damage responses [41,42]. Accumulating evidence indicate that RPA plays an active role in DNA damage responses beyond protection of ssDNA sequences from degradation by nucleases. For example, RPA inhibits APE1's cleavage of the AP site in ssDNA without requiring direct protein-protein interaction [43]. On the other hand, human nuclear uracil-DNA glycosylase (UNG2) individually interacts with PCNA and RPA and colocalizes with these proteins in replication foci. Phosphorylated UNG2 is present in these foci [44]. The S-phase-specific of UNG2-RPA complex was suggested to be involved in post-replicative repair of U misincorporated in nascent DNA [45]. In this study, we show that NEIL1 and RPA are present in a nuclear complex and NEIL1 directly interacts with RPA *in vitro*. Additionally, RPA inhibits NEIL1's excision of 5-OHU when present in the single-strand segment of a partial duplex oligo resembling primer-template, but it stimulates NEIL1 to repair the lesion when present in the duplex sequence. RPA passively inhibits NEIL1 single-strand lesion excision activity but interacts with the glycosylase for stimulating its double-strand-specific activity, and PCNA is specific for specifically relieving inhibition by RPA but not by *E. coli* single-strand DNA binding protein (SSB). These results suggest an active role of RPA in controlling NEIL1-dependent repair of oxidative base damage in the replicating genome.

2. Materials and Methods

2.1. Oligonucleotide substrates

A 51-mer oligo containing 5-OHU at position 26 from the 5′-end or undamaged 51-mer control oligo contained C at position 26 were ^{32}P-labeled at the 5′ terminus with [γ-^{32}P] ATP using T4-PNK prior to annealing when necessary, as described earlier [23]. The sequences in complementary oligos had G opposite the lesion which was used for generating complete or partial duplexes at the 3′ end to produce 3′ primer-template structures as shown in Table 1. To generate the 5′ primer-template structure with reverse orientation the complementary oligo was shortened at the 5′ end. For optimal annealing, equimolar mixtures of lesion-containing and complementary strands were heated at 94°C for 2 min in PBS, and then slowly cooled to room temperature.

2.2. Plasmids

Mammalian expression plasmids for C-terminally FLAG-tagged NEIL1 were previously described [27]. Ectopic FLAG-NEIL1 in stably transfected cells and endogenous NEIL1 are expressed at comparable levels in the log-phase. Construction of *E. coli* expression plasmids for the wild type (WT) and truncated forms of NEIL1 and for the production of N-terminal GST-fusion NEIL1 C-terminal domain were described previously [26]. The expression plasmid for RPA (gift from Dr. M. E. Sukhodolets) is tricistronic encoding all three subunits [46]. This smallest subunit contains the N-terminal His-tag used for purification of the native heterotrimeric protein.

2.3. Expression and purification of recombinant proteins

Recombinant WT NEIL1 and truncated NEIL1 polypeptides were purified to homogeneity from *E. coli* as described previously [20,47]. His-tagged RPA was purified on a Ni^{2+} column followed by chromatography on a HiTrap-SP column (GE Healthcare). The GST-fused NEIL1 domains (289–349) and (289–389) as well as PCNA were expressed and purified as previously described [25].

2.4. Co-immunoprecipitation assay

The human HeLa S3 cells grown in DMEM at 37°C, 5% CO_2 were transfected with 2 μg empty FLAG or NEIL1-FLAG plasmids using lipofectanine. The cells were collected 48 h later, and lysed in buffer (20 mM Tris-HCl, pH 7.5, 150 mM NaCl, 1 mM EDTA, 1% Triton X-100, and 1 mM NaF, 1 mM Na-orthovanadate, β-mercaptoethanol, plus protease inhibitors). In one experiment, the cells were treated with antimycin A (25 μM) for 1 h to induce oxidative stress prior to harvesting. In some experiments the cell lysates were digested with 500 units/ml DNase I (Ambion) at 37°C for 1 h, and cleared by centrifugation as previously described [25]. The lysates were then immunoprecipitated for 3 h at 4°C with FLAG M2 antibody agarose beads (Sigma). The beads were collected by centrifugation, washed three times with cold TBS, and the FLAG immunocomplex was eluted from the beads by adding SDS loading buffer, and separated by SDS-PAGE for immunoblot analysis.

2.5. In vitro pulldown assay

Wild type NEIL1 or its truncated mutants (5 pmol) were incubated with His-tagged RPA (5 pmol) in 0.5 ml TBS for 1 h at 4°C and then mixed with HIS-Select HC nickel beads (Sigma) with constant rotation for 1 h at 4°C. The beads were then washed extensively with wash buffer (50 mM Tris-HCl, pH 7.5, 500 mM NaCl). After elution of the proteins with SDS sample buffer and SDS-PAGE, the presence of interacting proteins was tested by immunoblotting.

GST pull down assays were performed as described previously [48]. Briefly, proteins mixed with glutathione-sepharose beads (20 μl) alone or bound to GST-tagged truncated NEIL1 domains (312–349 and 312–389) (10 pmol) were incubated with RPA or PCNA (2.5 pmol each) in 0.5 ml. After washing, the bound proteins were separated by SDS-PAGE followed by immunoblotting.

2.6. Far Western analysis

The interacting proteins (40 pmol) were separated by SDS-PAGE and transferred to nitrocellulose membranes. All subsequent steps were performed as described previously [20] with only slight modifications. The membrane was probed with either RPA or NEIL1 (10 pmol/ml) in PBS supplemented with 0.5% NFDM, 0.05% Tween 20, 10 mM trimethylamine-N-oxide (TMAO) and 1mM DTT for 4h followed by washing. Immunoblot analysis was then performed to detect interaction.

2.7. Fluorescence analysis

Interaction of RPA with NEIL1 C-terminal peptide (residues 312–349, lacking aromatic amino acids) was monitored in an LS50 spectrofluorimeter (Perkin Elmer) by the decrease in intrinsic tryptophan fluorescence of RPA (λ_{ex} = 295, λ_{em} = 300–450 nm) upon titration. For all binding experiments, the proteins were incubated in 10 mM PBS (150 mM NaCl), pH 7.5, 5% glycerol and incubated at 25°C for 5 min. The binding constant K_D was calculated by plotting ΔF (change in RPA fluorescence at 345 nm) versus ligand concentration according to the equation $\Delta F = \Delta F_{max} \cdot [ligand]/K_D + [ligand]$.

2.8. Assay of DNA glycosylase activity

NEIL1's DNA glycosylase activity was quantitated by strand incision at the 5-OHU site as previously described [25] with following modifications. When appropriate, the substrate oligo (25 nM) was preincubated with RPA (as indicated) for 15 min at 4°C in a 10 μl reaction mixture containing 40 mM HEPES-KOH, pH 7.5, 50 mM KCl, 1 mM $MgCl_2$, and appropriate amount of bovine serum albumin (BSA) to maintain a constant protein level prior to addition of NEIL1 and incubation at 37°C. The reaction was stopped after 10 min with 70% formamide/30 mM NaOH. The intact and cleaved oligos were then separated by denaturing gel electrophoresis in 20% polyacrylamide containing 7M urea, 90 mM Tris-borate (pH 8.3) and 2 mM EDTA, and the radioactivity in the DNA bands was quantitated in a PhosphorImager using ImageQuant software and the data presented using SigmaPlot.

2.9. Electrophoretic gel mobility shift analysis (EMSA)

The 5′ ^{32}P-labeled 51-mer oligo containing 5-OHU or C annealed to various complementary sequences (Table 1) were used. The DNA (25 nM) was then incubated with various amounts of RPA (as indicated) for 30 min at 4°C in a buffer containing 40 mM HEPES (pH 7.5), 50 mM KCl, 15% glycerol and appropriate amount of BSA to maintain an equal amount of total protein in each 20 μL reaction. Electrophoresis was performed at 4°C in 6% nondenaturing polyacrylamide gels in Tris-borate-EDTA buffer (pH 7.5 or 8.3), the protein-DNA complexes were visualized using a PhosphorImager and ImageQuant software.

3. Results

3.1. In vivo Association of NEIL1 with RPA

We recently documented physical and functional interaction of NEIL1 with PCNA, FEN1 and WRN as well as its *in vivo* association with RFC [24–26]. Furthermore, we also identified RPA among the proteins present in the NEIL1 immunoprecipitate in our screen for replication-associated proteins (Fig. 1A), suggesting stable association between RPA and NEIL1. We tested the effect of induced oxidative stress caused by the mitochondrial complex III inhibitor antimycin A, on RPA-association in NEIL1 immunocomplex. The level of both RPA1 and RPA2 in the NEIL1-FLAG IP increased after antimycin A treatment (Fig. 1B). We did not test for the presence of RPA3. While it is possible that the enhanced complex formation is due to RPA2 phosphorylation, it is also possible, in analogy with UNG2 phosphorylation in replication foci, that NEIL1 is phosphorylated or otherwise covalently modified in the stressinduced complex [45]. That the amount of PCNA and FEN1 also increased in the NEIL1 IP after oxidative stress supports the possibility that the increased level of NEIL1 complex was generated to meet the need for repairing additional base lesions generated by ROS. However, we did not observe any change in NEIL1 association with RFC1 (Figure 1B).

Because both RPA and NEIL1 have intrinsic affinity for DNA, we considered the possibility that the association of RPA and NEIL1 was mediated by DNA. However, treatment of cell lysates with DNase I prior to co-immunoprecipitation did not affect the levels of RPA found

in the NEIL1 IP (Figure 1C). Hence, we concluded that NEIL1's association with RPA is not DNA-mediated in human cells.

3.2. Mapping the RPA interaction site to NEIL1's C-terminal region

Commensurate with its multiple roles in various DNA metabolic pathways, RPA interacts with a large number of partner proteins primarily via RPA1 and RPA2 subunits. We confirmed the stable binary interaction between NEIL1 and RPA in the absence of DNA using purified recombinant proteins. Far Western analysis indicated that NEIL1 interacted with 70 kDa RPA1 in a dose-dependent fashion, while no interaction was observed with RPA2, RPA3 or the BSA control (Fig. 2A, left panel). Although the recombinant WT RPA like the endogenous protein contains RPA3 (Fig. 2C), we did not test for the presence of RPA3 in these studies. We should however point out that while Far Western analysis did not show NEIL1's interaction with RPA2 (which was present in the WT protein), we cannot exclude the possibility that such interaction was not detected by such analysis which requires refolding of RPA2 *in situ* on the membrane. In addition, we observed that the NEIL1 CΔ40 mutant had lower affinity for binding to the native RPA than the WT protein (Fig. 2A, right panel). A similar experiment showed no interaction of native RPA with the NEIL1 CΔ101 mutant (data not shown) confirming that NEIL1's common interaction domain near the C-terminus that is used for its association with other proteins is also used in interaction with RPA [20,24–27].

We confirmed the Far Western results using both His- and GST-tag pull-down analyses. Co-elution of NEIL1 and NEIL1 CΔ40 but not NEIL1 CΔ101 with His-tagged RPA (His-tag in RPA1) confirmed the interaction interface as being within residues 289–349 of NEIL1 (Fig. 2B, lanes 3–5). WT NEIL1 in the absence of His-tag RPA was used as a control (Fig. 2B, lane 2). We further mapped NEIL1's interacting region for RPA using GST-tagged nested deletion mutants. In addition to WT and NEIL1 CΔ40, we observed stable interaction of RPA with NEIL1 C-terminal domains consisting of residues 289–389, 289–349 and 312–389 (Fig. 3A). However, the 1–311 truncated protein (CΔ78 mutant) did not bind to RPA suggesting its lack of interaction domain. However, the fragment containing aa residues 312–349 did not show interaction with RPA (lane 8) which could be due to the lack of its proper refolding on the membrane. To confirm that the minimal interaction interface for RPA encompasses residues 312–349 in NEIL1 (with possible involvement of additional residues in the surrounding sequences), we performed co-elution analysis of RPA with GST-fused C-terminal peptides of NEIL1, which showed that residues 289–349 and 312–349 of NEIL1 were indeed sufficient for interaction (Fig. 3B, lane 2, top panel). In contrast, weaker binding of PCNA but not RPA to the peptide with residues 312–349 compared to that containing residues 289–349 (Fig. 3B, lane 2 versus 1, bottom panel), supported our previous study showing that the KA box motif, included in residues 289–311 of NEIL1 but in the 312–349 fragment, is important for NEIL1-PCNA interaction but not for RPA binding [25]. Thus, while the minimal interaction domain is common for NEIL1's interaction with RPA and PCNA, additional residues unique to each interacting partner are required that may modulate its affinity.

3.3. Binding affinity analysis

We utilized intrinsic fluorescence of RPA to calculate its affinity for NEIL1's common interaction domain (residues 312–349) that lacks aromatic amino acid residues. The RPA fluorescence decreased in a dose-dependent manner in the presence of this peptide suggesting localized conformation change after binding to the peptide (Fig. 4). As predicted, the NEIL1 peptide itself had negligible fluorescence (Fig. 4 upper panel). The calculated apparent dissociation constant (K_D) of approximately 20 nM (Fig. 4, lower panel) indicates strong affinity of the minimum interacting peptide.

3.4. Substrate structure-dependent regulation of NEIL1 activity by RPA

We investigated NEIL1's glycosylase/AP lyase activity with RPA-bound partial duplex oligonucleotide substrates with various lengths single-stranded regions simplistically representing chain elongation by the replicating DNA polymerase (Table 1). In these substrates, the damage (5-OHU) is considered to be generated *in situ* in the template strand. Comparing the effect of increasing molar ratio of RPA to the substrate DNA we observed significant inhibition of NEIL1 activity when the lesion was located in the single-stranded region of RPA-bound DNA (Fig. 5, left panel). The level of inhibition correlated with two variables, the increase in RPA to DNA ratio and the distance of the lesion from the primer-template junction. The farther the lesion is located from this junction, the higher was the inhibition at the same molar ratio of RPA and NEIL1. On the other hand, RPA stimulated NEIL1 activity more than 2-fold when the lesion was located within the duplex region of the substrate (Fig. 6). We then tested the activity of the NEIL1 1–311 truncation mutant with these substrates, which showed no interaction with RPA (Fig. 5, right panel). A nearly identical pattern of inhibition was seen when the lesion was in the single-stranded or primer-template junction regions. However, unlike for WT NEIL1, RPA had no stimulatory effect on the activity of the NEIL1 1–311 mutant when the lesion was located in the duplex sequence. At the same time, RPA did not inhibit the activity with the duplex DNA substrate presumably because of the lack of binding (Fig. 6). As a control, we confirmed that RPA itself had no cleavage activity for any of these 5-OHU-containing substrates (data not shown). Our results thus suggest that RPA inhibits NEIL1 activity passively on the ssDNA substrate while its physical interaction, like that of FEN1 and PCNA, enhances NEIL1's activity with duplex DNA substrates.

3.5. Effect of strand polarity on RPA inhibition of NEIL1

We then determined the extent of RPA inhibition on NEIL1 activity using either a 3′ primer-template or 5′ primer-template mimicking partial duplex with the lesion placed near the ss-duplex junction. These two substrates are nearly identical except for the polarity of the strand containing the lesion with respect to the duplex segment, as schematically shown in Fig. 7. We observed inhibition of both NEIL1 and NEIL1 1–311 truncation mutant with both substrates and at the highest RPA:DNA ratio the inhibition level was comparable for these substrates (Fig. 7). However, at lower RPA concentration, inhibition was significantly greater with the 5′ primer-template relative to the 3′ primer-template substrate (Fig. 7). RPA has been shown to bind single-stranded DNA with a 5′ → 3′ polarity and in a sequential multi-step manner [35,36,49]. Our results thus suggest that RPA's preferred polarity for binding could affect its ability to regulate NEIL1 activity on lesions in ssDNA near the primer-template junction.

3.6. Gel mobility shift analysis of RPA binding

Our observation that the RPA's dose-dependent inhibition of NEIL1 1–311 was comparable to that of WT NEIL1 even in the absence of physical interaction, supports the likelihood that this inhibition is due to passive sequestration of the lesion from NEIL1. To test this further, we examined RPA's binding to ss and partial duplex oligos containing 5-OHU in the single-strand segment. NEIL1 activity was inhibited by RPA for all of these substrates (ssDNA, Rep15, Rep21 and Rep24). We observed multiple RPA-DNA complexes of different molecular size using gel shift analysis (Fig. 8). The larger, slower migrating complexes became more prominent with increasing RPA concentration. The smaller, faster migrating complexes were not present at higher RPA concentration. This suggests that the number of RPA molecules that bind to each oligo increases with increasing RPA concentration [50].

We also noted the absence of larger, slower migrating complexes correlating with the fewer nucleotides in the ss segment when compared with the 51-mer ss substrate (Fig. 8). We concluded that the fastest migrating band represents a single RPA molecule bound to DNA, with the addition of another RPA molecule in each subsequent band of decreased mobility

[50]. Four RPA molecules could maximally bind to a 51-mer oligonucleotide, as shown in previous studies characterizing different DNA binding modes of RPA [36,40,51]. These results support our model of dose-dependent inhibition of NEIL1 activity via steric hindrance by multiple RPA molecules bound to the substrate oligo without direct physical interaction.

3.7. PCNA relieves RPA inhibition of NEIL1 activity

We showed earlier that PCNA stimulated NEIL1 activity on substrates containing uncoated ssDNA, and also bubble or forked DNA structures [25]. Here we examined PCNA's ability to stimulate NEIL1 on RPA-coated linear primer-template oligo substrates. In this case, PCNA would load on the end, freely sliding on and off the duplex region of the substrate, so that in the presence of excess PCNA, equilibrium is maintained between bound and free PCNA. Fig. 9A shows that RPA inhibited NEIL1 activity on the Rep21 substrate in a dose-dependent manner as previously observed (lanes 3–5). Interestingly, NEIL1 activity was stimulated, as before, when PCNA was added to the reaction with low concentration of RPA (1.25:1 molar ratio; Fig. 9A, compare lanes 2 and 6). As the level of RPA was increased, NEIL1 stimulation by PCNA decreased to some extent. At the highest RPA concentration (5:1 molar ratio), it inhibited NEIL1 activity even in the presence of PCNA but to a much smaller extent than the absence of PCNA (compare lanes 4 and 8). These data suggest that PCNA and RPA may collaborate in regulating NEIL1 activity at the replication fork. To test that the PCNA reversal of RPA inhibition is specific, we investigated whether PCNA would relieve inhibition by *E. coli* ssDNA binding protein (SSB), which inhibited NEIL1 in the same manner as RPA but does not interact with NEIL1. PCNA did not restore NEIL1 activity inhibited by SSB (Fig. 9B). Taken together, these results confirm PCNA's active role in RPA inhibition of NEIL1 activity requires specific and cognate interactions.

4. Discussion

Because of NEIL1's S-phase-dependent upregulation and preference for ssDNA substrates [28,39], we have proposed its preferential role in repairing lesions in the replicating DNA. Unlike bulky adducts, oxidized bases do not block chain elongation by replicating DNA polymerases δ/ε [39,41,52]. Unrepaired lesions may be replicated by the replicative or translesion synthesis (TLS) polymerases to generate mutations. We have postulated that free DNA glycosylases or their complexes recruited at replication sites provide surveillance and repair oxidized bases in order to maintain genomic integrity. In support of this model, we have shown NEIL1's association with several replication-associated proteins including PCNA, FEN1, WRN, RFC, and 9-1-1 [24–27]. We have now shown that the NEIL1 immunocomplex isolated from human cells contained at least the large subunits of RPA (RPA1 and RPA2), and that this association increases under oxidative stress. Whether post-translational modification of NEIL1 and/or RPA occurring during oxidative stress is responsible for enhanced complex formation remains to be established.

The native heterotrimeric RPA is an indispensable component in various DNA transactions including replication, repair, cell cycle checkpoints and DNA damage responses [41–43]. While RPA's binding to ssDNA is essential for replication, recombination and repair making it a core component of these pathways [52], RPA is actively engaged in protein-protein interactions and recruitment of proteins to DNA damage sites in order to maintain the genome integrity by activating cellular stress responses.

We demonstrated direct binary interaction between NEIL1 and the large subunit (RPA1) in the absence of DNA, which is mediated via NEIL1's common interacting interface in the disordered C-terminal domain. RPA inhibits NEIL1 activity *in vitro* when the damage is present in the single-stranded region of a primer-template structure. The degree of inhibition decreases when the damage is closer to the primer-template junction suggesting that the lesion becomes

more accessible near the duplex region where RPA no longer coats the DNA. Interestingly, our observation that RPA stimulated WT NEIL1 for duplex DNA substrate, but not the 1–311 truncation mutant lacking the interaction interface suggests that direct physical interaction with RPA is critical for the stimulation but not inhibition of NEIL1's activity. The inhibition is likely to be due to the prevention of NEIL1's access to RPA-bound lesions. NEIL1's inhibition by *E. coli* SSB which does not interact with NEIL1 could be explained by such steric consideration. Our EMSA results showing RPA dose-dependent increase in the degree of ssDNA binding also support this scenario. We have confirmed previous observation of sequential multi-step binding of RPA to ssDNA and occlusion of 8–10, 12–23 or ~30 nucleotides by a single heterotrimeric RPA molecule with varying conformation [31,38,40,51,53]. The difference in the extent of inhibition of NEIL1 using 3′ vs. 5′ primer-template substrates at low RPA concentration but not at high concentration is consistent with these results. The EMSA data suggest that at low concentration only one or two RPA molecules are bound to a substrate molecule, and RPA exists in an extended conformation utilizing weaker DNA binding of DBD-C and -D. Thus NEIL1 is capable of competing with the weak binding for access to the lesion when they are bound near the primer-template junction, but not with DBD-A and –B with stronger binding. DBD (-A and -B) are the only domains bound to the DNA at higher RPA concentration.

RPA has been proposed to function as a DNA damage sensor in triggering various damage responses for oxidative damage [54]. It is likely that NEIL1 collaborates with RPA in surveillance of oxidatively generated base lesions in the single-stranded DNA template prior to replication. Our results supporting the existence of replication-associated repair of oxidized base lesion are similar to the studies on repair of U by UNG2 where the investigators showed association of UNG2 with PCNA and RPA [44,45]. They observed that UNG2 is phosphorylated when complexed with RPA. Whether NEIL1 is similarly phosphorylated or otherwise covalently modified to enhance its interaction with RPA and other replication-associated proteins after oxidative stress remain to be explored. However, those authors proposed post-replication repair of misincorporated U mediated by the UNG2 complexed with the replication machinery. On the contrary, we suggest that replication-associated repair of oxidative template lesions is essential in the prereplicative state in order to prevent mutation during synthesis.

Finally, we have shown that PCNA relieves RPA inhibition of NEIL1 in repairing a lesion located near the single-strand duplex junction. This suggests that NEIL1 repairs oxidized bases in concert with DNA replication by sharing replication-associated proteins including PCNA and RPA. It is likely that PCNA regulates NEIL1's activity on the replicating template in order to prevent double-strand breaks resulting from template strand cleavage by NEIL1.

Acknowledgments

We would like to thank Thomas Wood, Director of the Molecular Genetics Core, Alex Kurosky and Steven Smith of the Biomolecular Resources Facility at UTMB for various services and analysis, and Ms. Wanda Smith for expert secretarial assistance. Research was supported by USPHS grants R01 CA081063 (SM), R01 CA102271 (TKH), P01 CA092584 (SM) and the NIEHS Toxicology Center grant P30 ES06676. CAT was supported by a USPHS predoctoral training grant T32-07254.

Abbreviations used are

α	antibody
aa	amino acid
AP	abasic

APE	AP-endonuclease
AU	arbitrary units
BSA	bovine serum albumin
Co-IP	co-immunoprecipitation
DTT	dithiothretiol
DTT	dithiothretiol
EMSA	electrophoretic mobility shift analysis
FEN1	flap endonuclease 1
5-OHU	5-hydroxyuracil
IP	immunoprecipitate
Lig 1	DNA ligase I
Lig IIIα	DNA ligase IIIα
LP-BER	long patch base excision repair
NFDM	nonfat dried milk
nt	nucleotide
PBS	phosphate buffered saline
PCNA	proliferating cell nuclear antigen
Pol β	DNA polymerase beta
RPA	replication protein A
Pol δ	DNA polymerase delta
SN-BER	single nucleotide base excision repair
ss	single-stranded
SSB	*E. coli* single-stranded DNA binding protein
TBS	tris-buffered saline
WT	wild type

REFERENCES

1. Breen AP, Murphy JA. Reactions of oxyl radicals with DNA. Free Radic Biol Med 1995;18:1033–1077. [PubMed: 7628729]
2. Cadet JL, Brannock C. Free radicals and the pathobiology of brain dopamine systems. Neurochem Int 1998;32:117–131. [PubMed: 9542724]
3. Grisham MB, Hernandez LA, Granger DN. Xanthine oxidase and neutrophil infiltration in intestinal ischemia. Am J Physiol 1986;251:G567–G574. [PubMed: 3020994]
4. Ames BN, Shigenaga MK, Hagen TM. Oxidants, antioxidants, and the degenerative diseases of aging. Proc Natl Acad Sci U S A 1993;90:7915–7922. [PubMed: 8367443]
5. Bozner P, Grishko V, LeDoux SP, Wilson GL, Chyan YC, Pappolla MA. The amyloid beta protein induces oxidative damage of mitochondrial DNA. J Neuropathol Exp Neurol 1997;56:1356–1362. [PubMed: 9413284]
6. DeWeese TL, Shipman JM, Larrier NA, Buckley NM, Kidd LR, Groopman JD, Cutler RG, te Riele H, Nelson WG. Mouse embryonic stem cells carrying one or two defective Msh2 alleles respond

abnormally to oxidative stress inflicted by low-level radiation. Proc Natl Acad Sci U S A 1998;95:11915–11920. [PubMed: 9751765]

7. Meyer TE, Liang HQ, Buckley AR, Buckley DJ, Gout PW, Green EH, Bode AM. Changes in glutathione redox cycling and oxidative stress response in the malignant progression of NB2 lymphoma cells. Int J Cancer 1998;77:55–63. [PubMed: 9639394]
8. Mukherjee SK, Adams JD Jr. The effects of aging and neurodegeneration on apoptosis-associated DNA fragmentation and the benefits of nicotinamide. Mol Chem Neuropathol 1997;32:59–74. [PubMed: 9437658]
9. Multhaup G, Ruppert T, Schlicksupp A, Hesse L, Beher D, Masters CL, Beyreuther K. Reactive oxygen species and Alzheimer's disease. Biochem Pharmacol 1997;54:533–539. [PubMed: 9337068]
10. Krokan HE, Nilsen H, Skorpen F, Otterlei M, Slupphaug G. Base excision repair of DNA in mammalian cells. FEBS Lett 2000;476:73–77. [PubMed: 10878254]
11. Mitra S, Izumi T, Boldogh I, Bhakat KK, Hill JW, Hazra TK. Choreography of oxidative damage repair in mammalian genomes. Free Radic Biol Med 2002;33:15–28. [PubMed: 12086678]
12. Ikeda S, Biswas T, Roy R, Izumi T, Boldogh I, Kurosky A, Sarker AH, Seki S, Mitra S. Purification and characterization of human NTH1, a homolog of Escherichia coli endonuclease III. Direct identification of Lys-212 as the active nucleophilic residue. J Biol Chem 1998;273:21585–21593. [PubMed: 9705289]
13. Radicella JP, Dherin C, Desmaze C, Fox MS, Boiteux S. Cloning and characterization of hOGG1, a human homolog of the OGG1 gene of Saccharomyces cerevisiae. Proc Natl Acad Sci U S A 1997;94:8010–8015. [PubMed: 9223305]
14. Bandaru V, Sunkara S, Wallace SS, Bond JP. A novel human DNA glycosylase that removes oxidative DNA damage and is homologous to Escherichia coli endonuclease VIII. DNA Repair (Amst) 2002;1:517–529. [PubMed: 12509226]
15. Hazra TK, Izumi T, Boldogh I, Imhoff B, Kow YW, Jaruga P, Dizdaroglu M, Mitra S. Identification and characterization of a human DNA glycosylase for repair of modified bases in oxidatively damaged DNA. Proc Natl Acad Sci U S A 2002;99:3523–3528. [PubMed: 11904416]
16. Hazra TK, Kow YW, Hatahet Z, Imhoff B, Boldogh I, Mokkapati SK, Mitra S, Izumi T. Identification and characterization of a novel human DNA glycosylase for repair of cytosine-derived lesions. J Biol Chem 2002;277:30417–30420. [PubMed: 12097317]
17. Morland I, Rolseth V, Luna L, Rognes T, Bjoras M, Seeberg E. Human DNA glycosylases of the bacterial Fpg/MutM superfamily: an alternative pathway for the repair of 8-oxoguanine and other oxidation products in DNA. Nucleic Acids Res 2002;30:4926–4936. [PubMed: 12433996]
18. Takao M, Kanno S, Kobayashi K, Zhang QM, Yonei S, van der Horst GT, Yasui A. A back-up glycosylase in Nth1 knock-out mice is a functional Nei (endonuclease VIII) homologue. J Biol Chem 2002;277:42205–42213. [PubMed: 12200441]
19. Hill JW, Hazra TK, Izumi T, Mitra S. Stimulation of human 8-oxoguanine-DNA glycosylase by AP-endonuclease: potential coordination of the initial steps in base excision repair. Nucleic Acids Res 2001;29:430–438. [PubMed: 11139613]
20. Wiederhold L, Leppard JB, Kedar P, Karimi-Busheri F, Rasouli-Nia A, Weinfeld M, Tomkinson AE, Izumi T, Prasad R, Wilson SH, Mitra S, Hazra TK. AP endonuclease-independent DNA base excision repair in human cells. Mol Cell 2004;15:209–220. [PubMed: 15260972]
21. Tomkinson AE, Chen L, Dong Z, Leppard JB, Levin DS, Mackey ZB, Motycka TA. Completion of base excision repair by mammalian DNA ligases. Prog Nucleic Acid Res Mol Biol 2001;68:151–164. [PubMed: 11554294]
22. Podlutsky AJ, Dianova, Wilson SH, Bohr VA, Dianov GL. DNA synthesis and dRPase activities of polymerase beta are both essential for single-nucleotide patch base excision repair in mammalian cell extracts. Biochemistry 2001;40:809–813. [PubMed: 11170398]
23. Dou H, Mitra S, Hazra TK. Repair of oxidized bases in DNA bubble structures by human DNA glycosylases NEIL1 and NEIL2. J Biol Chem 2003;278:49679–49684. [PubMed: 14522990]
24. Das A, Boldogh I, Lee JW, Harrigan JA, Hegde ML, Piotrowski J, de Souza Pinto N, Ramos W, Greenberg MM, Hazra TK, Mitra S, Bohr VA. The human Werner syndrome protein stimulates repair of oxidative DNA base damage by the DNA glycosylase NEIL1. J Biol Chem 2007;282:26591–26602. [PubMed: 17611195]

25. Dou H, Theriot CA, Das A, Hegde ML, Matsumoto Y, Boldogh I, Hazra TK, Bhakat KK, Mitra S. Interaction of the human DNA glycosylase NEIL1 with proliferating cell nuclear antigen. The potential for replication-associated repair of oxidized bases in mammalian genomes. J Biol Chem 2008;283:3130–3140. [PubMed: 18032376]
26. Hegde ML, Theriot CA, Das A, Hegde PM, Guo Z, Gary RK, Hazra TK, Shen B, Mitra S. Physical and functional interaction between human oxidized base-specific DNA glycosylase neil1 and flap endonuclease 1. J Biol Chem. 2008
27. Guan X, Bai H, Shi G, Theriot CA, Hazra TK, Mitra S, Lu AL. The human checkpoint sensor Rad9-Rad1-Hus1 interacts with and stimulates NEIL1 glycosylase. Nucleic Acids Res 2007;35:2463–2472. [PubMed: 17395641]
28. Melendy T, Stillman B. An interaction between replication protein A and SV40 T antigen appears essential for primosome assembly during SV40 DNA replication. J Biol Chem 1993;268:3389–3395. [PubMed: 8381428]
29. Stillman B, Bell SP, Dutta A, Marahrens Y. DNA replication and the cell cycle. Ciba Found Symp 1992;170:147–156. discussion 156–160. [PubMed: 1336449]
30. Waga S, Bauer G, Stillman B. Reconstitution of complete SV40 DNA replication with purified replication factors. J Biol Chem 1994;269:10923–10934. [PubMed: 8144677]
31. Deng X, Habel JE, Kabaleeswaran V, Snell EH, Wold MS, Borgstahl GE. Structure of the full-length human RPA14/32 complex gives insights into the mechanism of DNA binding and complex formation. J Mol Biol 2007;374:865–876. [PubMed: 17976647]
32. Richard DJ, Bolderson E, Cubeddu L, Wadsworth RI, Savage K, Sharma GG, Nicolette ML, Tsvetanov S, McIlwraith MJ, Pandita RK, Takeda S, Hay RT, Gautier J, West SC, Paull TT, Pandita TK, White MF, Khanna KK. Single-stranded DNA-binding protein hSSB1 is critical for genomic stability. Nature 2008;453:677–681. [PubMed: 18449195]
33. Binz SK, Sheehan AM, Wold MS. Replication protein A phosphorylation and the cellular response to DNA damage. DNA Repair (Amst) 2004;3:1015–1024. [PubMed: 15279788]
34. Gomes XV, Wold MS. Functional domains of the 70-kilodalton subunit of human replication protein A. Biochemistry 1996;35:10558–10568. [PubMed: 8756712]
35. de Laat WL, Appeldoorn E, Sugasawa K, Weterings E, Jaspers NG, Hoeijmakers JH. DNA-binding polarity of human replication protein A positions nucleases in nucleotide excision repair. Genes Dev 1998;12:2598–2609. [PubMed: 9716411]
36. Iftode C, Borowiec JA. 5' --> 3' molecular polarity of human replication protein A (hRPA) binding to pseudo-origin DNA substrates. Biochemistry 2000;39:11970–11981. [PubMed: 11009611]
37. Bastin-Shanower SA, Brill SJ. Functional analysis of the four DNA binding domains of replication protein A. The role of RPA2 in ssDNA binding. J Biol Chem 2001;276:36446–36453. [PubMed: 11479296]
38. Arunkumar AI, Stauffer ME, Bochkareva E, Bochkarev A, Chazin WJ. Independent and coordinated functions of replication protein A tandem high affinity single-stranded DNA binding domains. J Biol Chem 2003;278:41077–41082. [PubMed: 12881520]
39. Wyka IM, Dhar K, Binz SK, Wold MS. Replication protein A interactions with DNA: differential binding of the core domains and analysis of the DNA interaction surface. Biochemistry 2003;42:12909–12918. [PubMed: 14596605]
40. Jiang X, Klimovich V, Arunkumar AI, Hysinger EB, Wang Y, Ott RD, Guler GD, Weiner B, Chazin WJ, Fanning E. Structural mechanism of RPA loading on DNA during activation of a simple pre-replication complex. Embo J 2006;25:5516–5526. [PubMed: 17110927]
41. Haring SJ, Mason AC, Binz SK, Wold MS. Cellular functions of human RPA1. Multiple roles of domains in replication, repair, and checkpoints. J Biol Chem 2008;283:19095–19111. [PubMed: 18469000]
42. Zou Y, Liu Y, Wu X, Shell SM. Functions of human replication protein A (RPA): from DNA replication to DNA damage and stress responses. J Cell Physiol 2006;208:267–273. [PubMed: 16523492]
43. Fan J, Matsumoto Y, Wilson DM 3rd. Nucleotide sequence and DNA secondary structure, as well as replication protein A, modulate the single-stranded abasic endonuclease activity of APE1. J Biol Chem 2006;281:3889–3898. [PubMed: 16356936]

44. Otterlei M, Warbrick E, Nagelhus TA, Haug T, Slupphaug G, Akbari M, Aas PA, Steinsbekk K, Bakke O, Krokan HE. Post-replicative base excision repair in replication foci. Embo J 1999;18:3834–3844. [PubMed: 10393198]
45. Hagen L, Kavli B, Sousa MM, Torseth K, Liabakk NB, Sundheim O, Pena-Diaz J, Otterlei M, Horning O, Jensen ON, Krokan HE, Slupphaug G. Cell cycle-specific UNG2 phosphorylations regulate protein turnover, activity and association with RPA. Embo J 2008;27:51–61. [PubMed: 18079698]
46. Sukhodolets KE, Hickman AB, Agarwal SK, Sukhodolets MV, Obungu VH, Novotny EA, Crabtree JS, Chandrasekharappa SC, Collins FS, Spiegel AM, Burns AL, Marx SJ. The 32-kilodalton subunit of replication protein A interacts with menin, the product of the MEN1 tumor suppressor gene. Mol Cell Biol 2003;23:493–509. [PubMed: 12509449]
47. Hazra TK, Mitra S. Purification and characterization of NEIL1 and NEIL2, members of a distinct family of mammalian DNA glycosylases for repair of oxidized bases. Methods Enzymol 2006;408:33–48. [PubMed: 16793361]
48. Das A, Wiederhold L, Leppard JB, Kedar P, Prasad R, Wang H, Boldogh I, Karimi-Busheri F, Weinfeld M, Tomkinson AE, Wilson SH, Mitra S, Hazra TK. NEIL2-initiated, APE-independent repair of oxidized bases in DNA: Evidence for a repair complex in human cells. DNA Repair (Amst) 2006;5:1439–1448. [PubMed: 16982218]
49. Kolpashchikov DM, Khodyreva SN, Khlimankov DY, Wold MS, Favre A, Lavrik OI. Polarity of human replication protein A binding to DNA. Nucleic Acids Res 2001;29:373–379. [PubMed: 11139606]
50. Fanning E, Klimovich V, Nager AR. A dynamic model for replication protein A (RPA) function in DNA processing pathways. Nucleic Acids Res 2006;34:4126–4137. [PubMed: 16935876]
51. Cai L, Roginskaya M, Qu Y, Yang Z, Xu Y, Zou Y. Structural characterization of human RPA sequential binding to single-stranded DNA using ssDNA as a molecular ruler. Biochemistry 2007;46:8226–8233. [PubMed: 17583916]
52. Wold MS. Replication protein A: a heterotrimeric, single-stranded DNA-binding protein required for eukaryotic DNA metabolism. Annu Rev Biochem 1997;66:61–92. [PubMed: 9242902]
53. Bochkareva E, Korolev S, Lees-Miller SP, Bochkarev A. Structure of the RPA trimerization core and its role in the multistep DNA-binding mechanism of RPA. Embo J 2002;21:1855–1863. [PubMed: 11927569]
54. Wood RD. DNA damage recognition during nucleotide excision repair in mammalian cells. Biochimie 1999;81:39–44. [PubMed: 10214908]

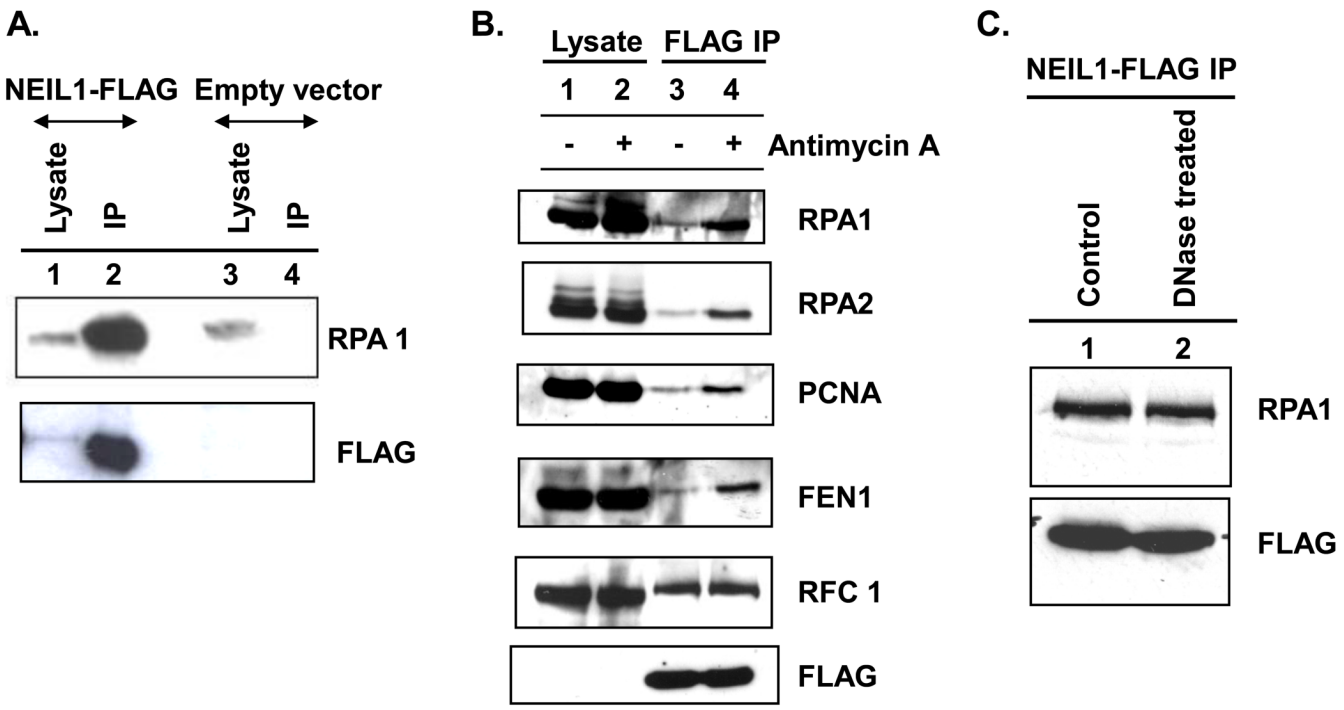

Figure 1. Oxidative stress-mediated increase in the levels of RPA, PCNA and FEN1 in NEIL1-FLAG IP

A. Western analysis of endogenous RPA in the NEIL1-FLAG (lanes 1 & 2) or empty-FLAG (lanes 3 & 4) immunoprecipitate (IP). Top panel: Detection of RPA in the lysate (lanes 1 & 3) and FLAG IP (lanes 2 & 4). Bottom panel: Western analysis of FLAG showing presence or absence of FLAG-tagged NEIL1. The small FLAG peptide in the empty vector was eluted from the gel. **B.** Western analysis of replication-associated proteins in the NEIL1-FLAG IP isolated from untreated (lane 3) or Antimycin A-treated cells (lane 4). Equal amounts of cell lysate proteins (10% of total lysate) from treated or non-treated cells were loaded in lanes 1 and 2. **C.** Immunoblot analysis for the detection of RPA in untreated NEIL1-FLAG IP (lane 1) or IP pretreated with DNase I (500 units/mL) for 1 h to remove contaminating genomic DNA. Lower panel: comparable FLAG NEIL1 levels in treated vs. untreated samples.

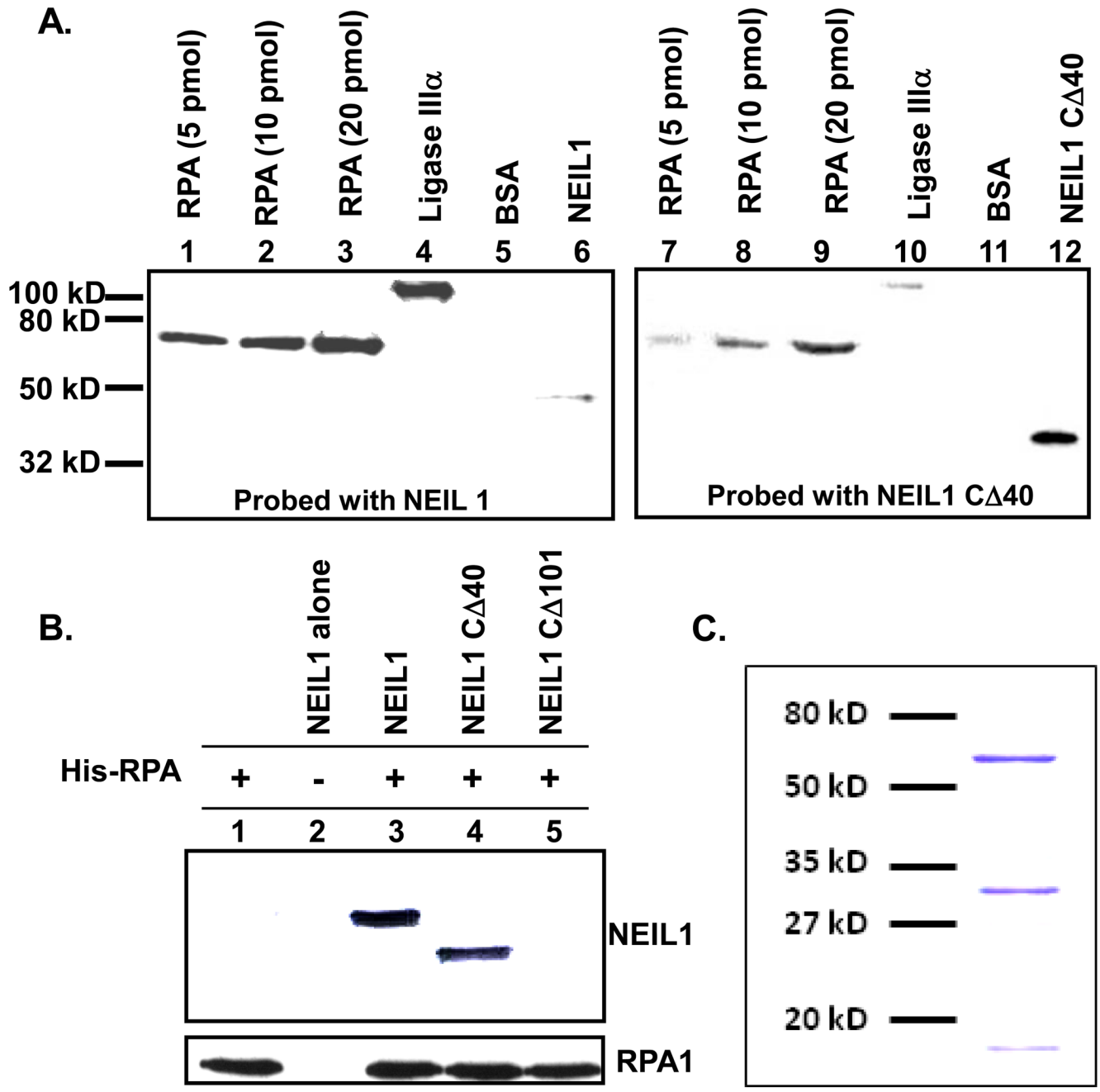

Figure 2. Mapping NEIL1's RPA-interacting segment

A. Left panel: Membrane immobilized RPA (lanes 1–3), Ligase IIIα (lane 4) and BSA (lane 5) were incubated with WT NEIL1 (10 pmol/mL) followed by immunological detection of NEIL1. RPA protein levels are shown, 20 pmol; Lig IIIa and BSA each, and 2 pmol of WT NEIL1 (lane 6) or NEIL CΔ40 (lane 12) were used. The membrane was probed with 10 pmol/mL WT NEIL1 or NEIL CΔ40 followed by immunological identification. **B.** His-tag pull-down of WT (lane 3) and deletion mutants (lanes 4 & 5) with His-tagged RPA. His-RPA alone (lane 1) and WT NEIL1 alone (lane 2) as controls. Top panel, immunoblot with α-NEIL1, bottom immunoblot with α-RPA. **C.** SDS-PAGE of purified recombinant RPA containing 70 kDa, 32 kDa and 14 kDa subunits.

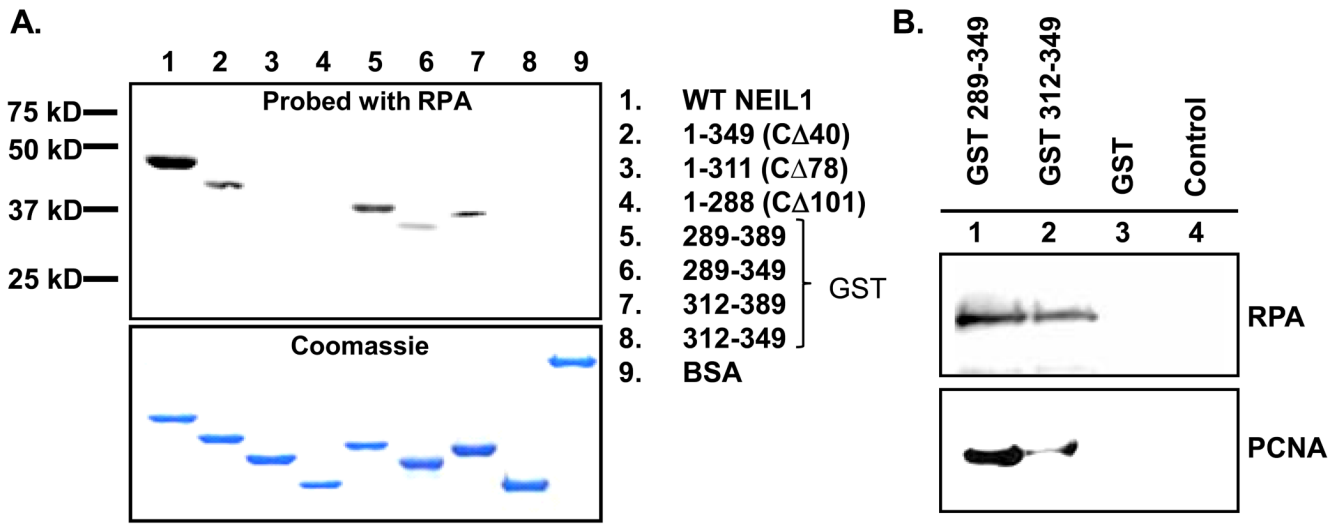

Figure 3. Co-elution of RPA and NEIL1

A. MappingNEIL1's C-terminal interaction domain for RPA interaction. Far Western analysis of RPA interaction with WT NEIL1 (lane 1), deletion mutants of NEIL1 (lanes 2–4) or GST-fused C-terminal domains of NEIL1 (lanes 5–8). Top panel: Far Western analysis probing with RPA. Bottom panel: Coomassie staining after SDS-PAGE. **B.** Co-elution analysis of RPA (top panel) or PCNA (bottom panel) with GST-tagged C-terminal segments of NEIL1 (lanes 1 and 2) coupled to glutathione-Sepharose beads. GST alone (lane 3) and beads alone (lane 4) serve as controls for nonspecific binding.

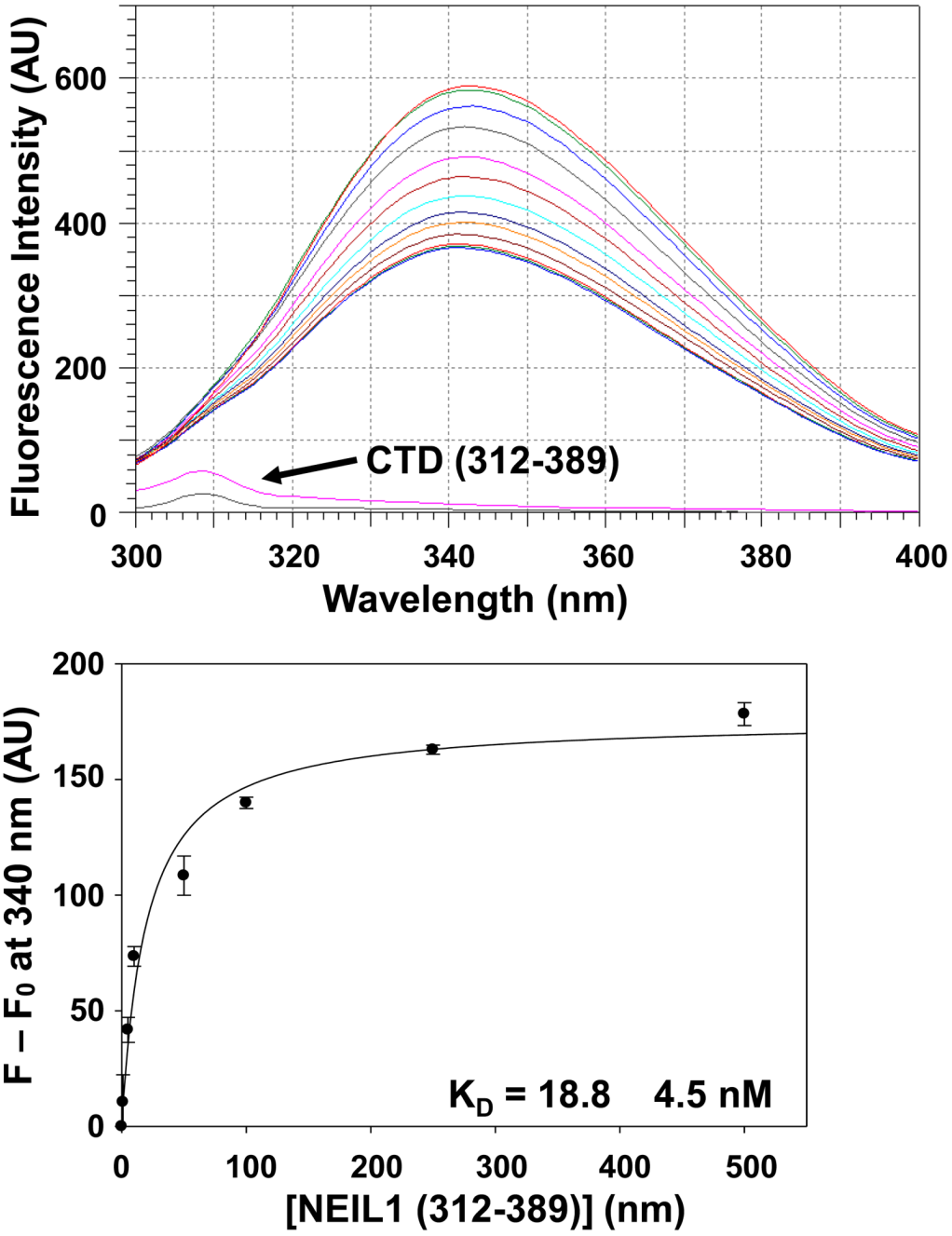

Figure 4. Intrinsic fluorescence analysis of RPA titrated with NEIL1's interacting domain

Top Panel: Tryptophan fluorescence spectra of RPA titrated with NEIL1 peptide (residues 312–349), change in RPA's intrinsic fluorescence intensity at 340 nM in the presence of the NEIL1 peptide.

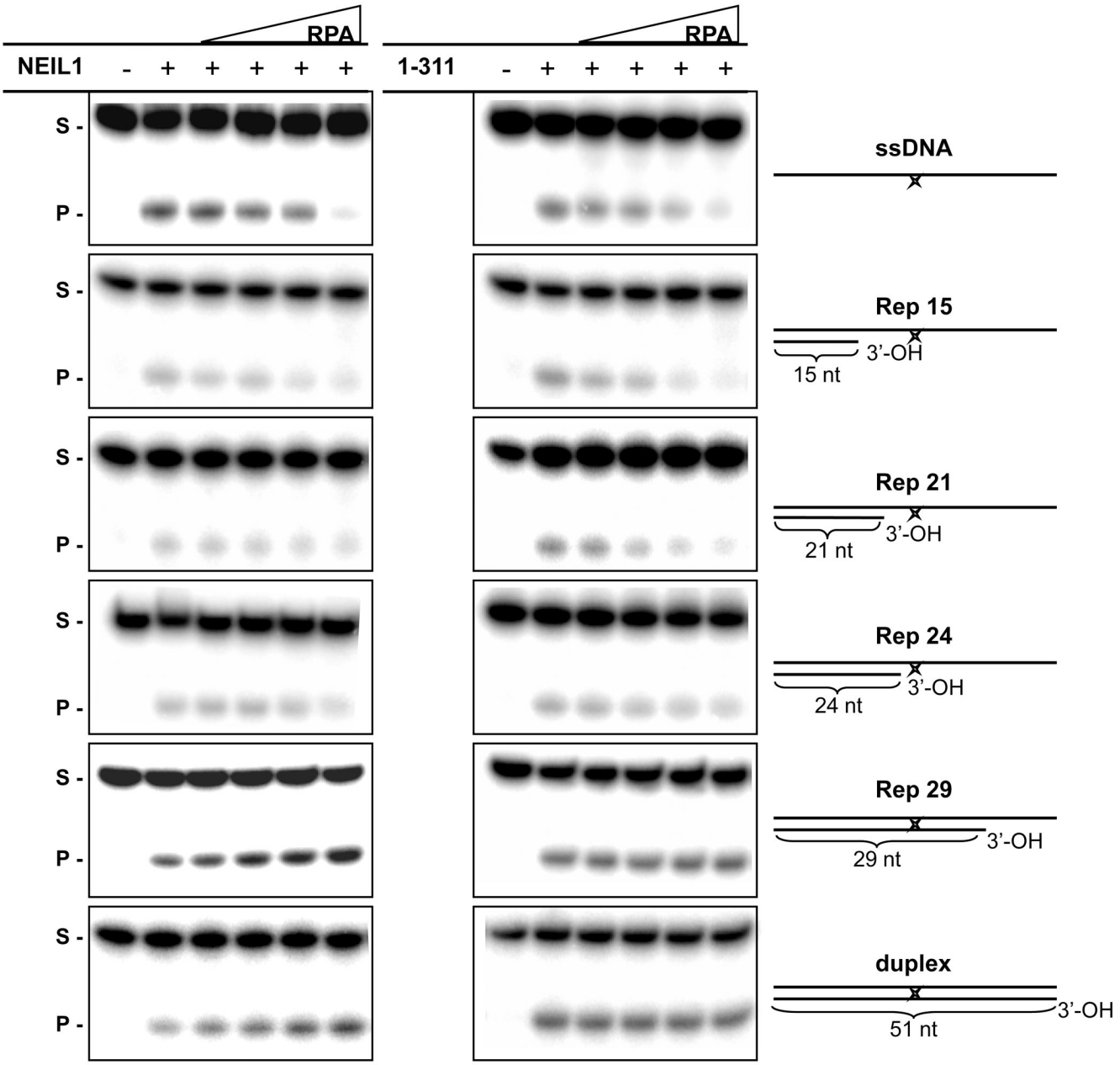

Figure 5. Effect of RPA on NEIL1 excision of 5-OHU from various DNA structures

A 51-mer 5-OHU-containing oligonucleotide (25nM) was used alone (single-stranded) or annealed with complementary strands to generate various primer-template structures (Table 5.1). The NEIL1 activity was measured, as described in Experimental Procedures, using WT NEIL1 (1 nM; left panel) or NEIL1 1–311 (right panel) alone or after preincubation of the DNA with an increasing RPA:DNA molar ratio (1.25:1, 2.5:1, 5:1 or 10:1). S and P indicate uncleaved substrate and cleaved product, respectively.

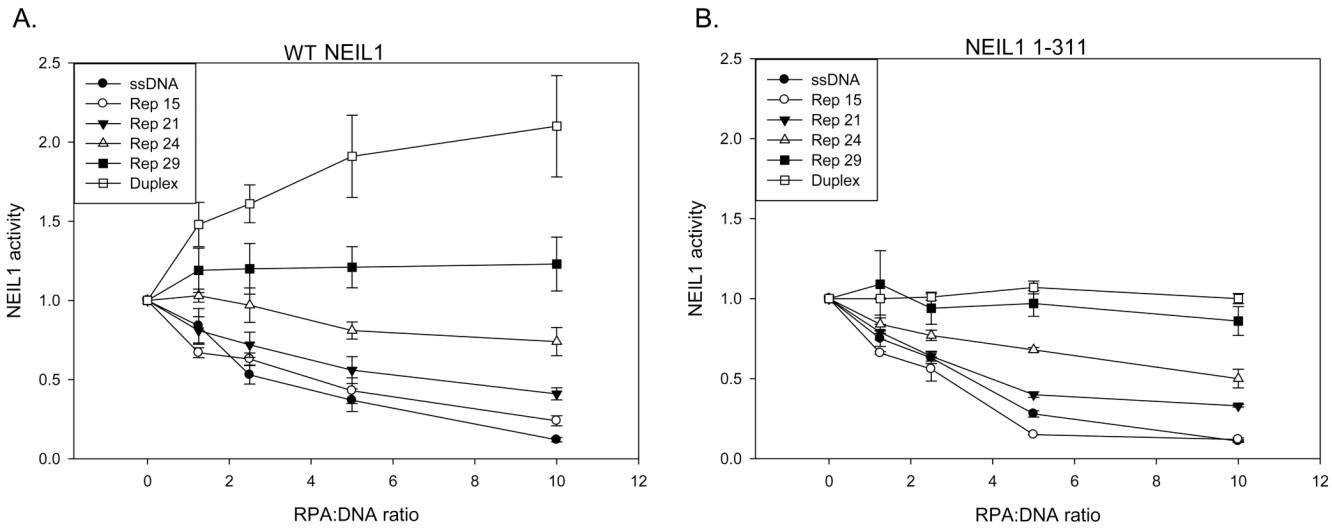

Figure 6. RPA inhibits NEIL1 5-OHU cleavage activity

The fold change in NEIL1 activity (**A**) or NEIL1 1–311 mutant (**B**) on various DNA substrates is plotted as a function of RPA:DNA molar ratio. Each point is the average of at least 3 experiments and error bars represent the standard deviation from the mean. Representative gels for both NEIL1 and NEIL1 1–311 are shown in Fig. 5.

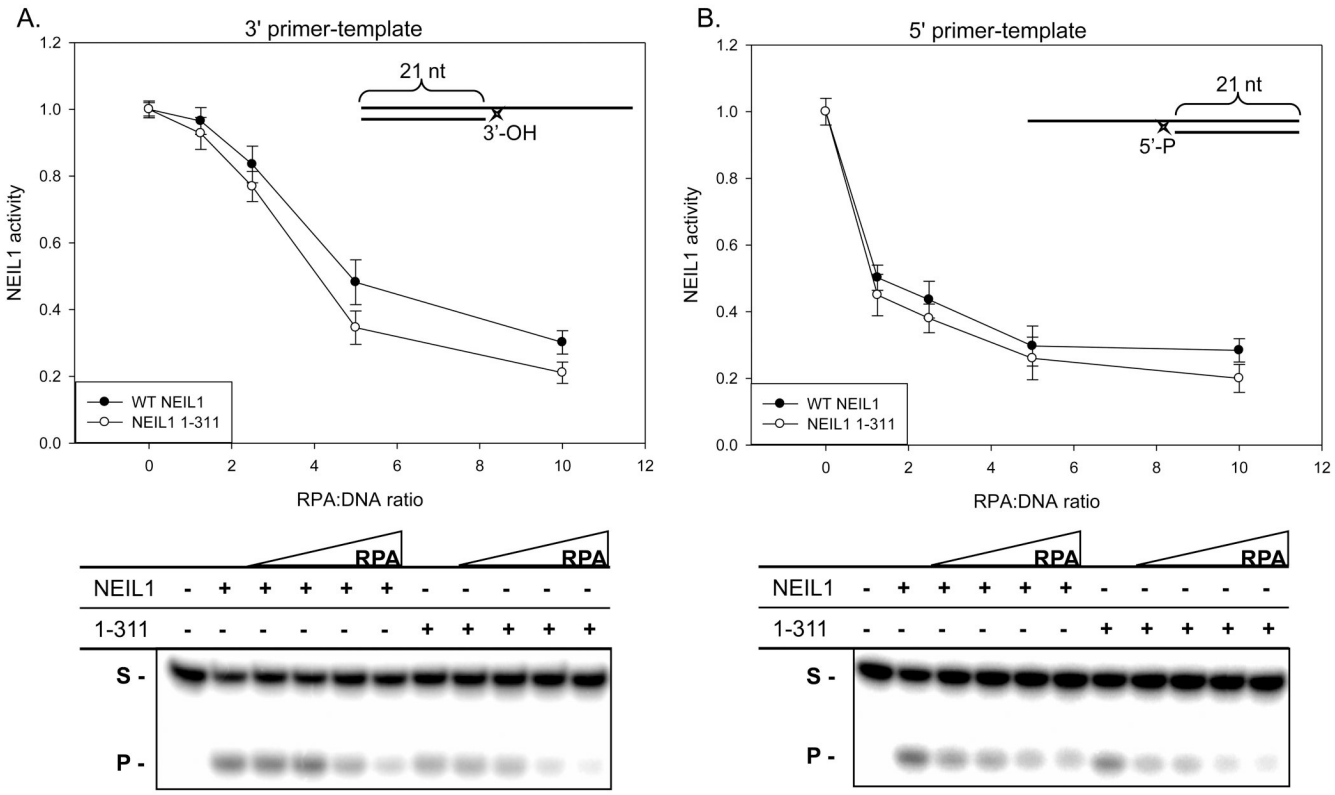

Figure 7. RPA Inhibition of NEIL1 activity on 3′ vs. 5′ primer-template substrates

Effect of RPA on full-length NEIL1 or NEIL1 1–311 cleavage of 25 nM 5-OHU containing 3′ primer-template substrate (**A**) or 5′ primer-template substrate (**B**). Top panel: Change in NEIL1 activity as a function of RPA:DNA molar ratio. Bottom panel: Representative gel of NEIL1 (1 nM) and NEIL1 1–311 (1 nM) activity alone or in the presence of RPA. Error bars represent standard error.

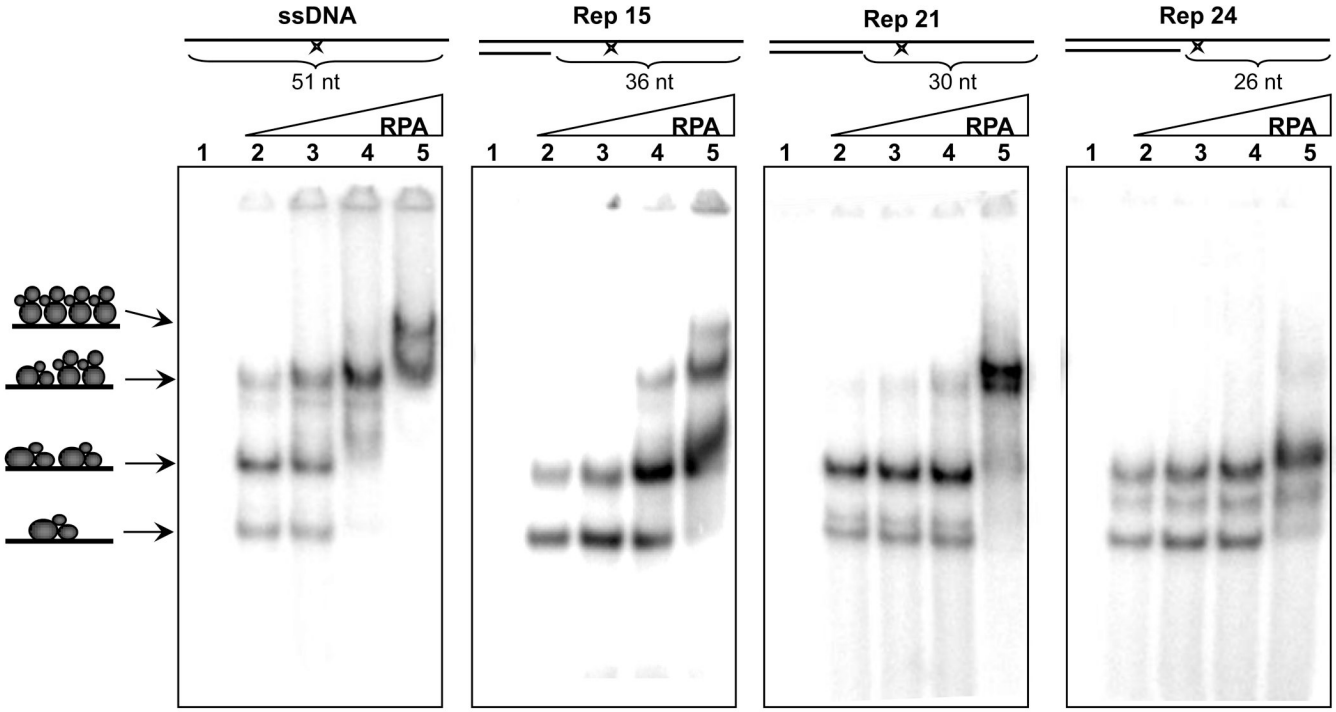

Figure 8. Effect of single-stranded DNA length in primer-template substrates on RPA binding

EMSA of no enzyme (lane 1) or increasing ratio of RPA to DNA (1.25:1, 2.5:1, 5:1 or 10:1; lanes 2–5) using the indicated DNA oligonucleotide substrate (25 nM). RPA was incubated at 4°C for 30 min in a 20 μL reaction prior to native gel electrophoresis at pH 8.3. The position of various RPA-DNA complexes is indicated.

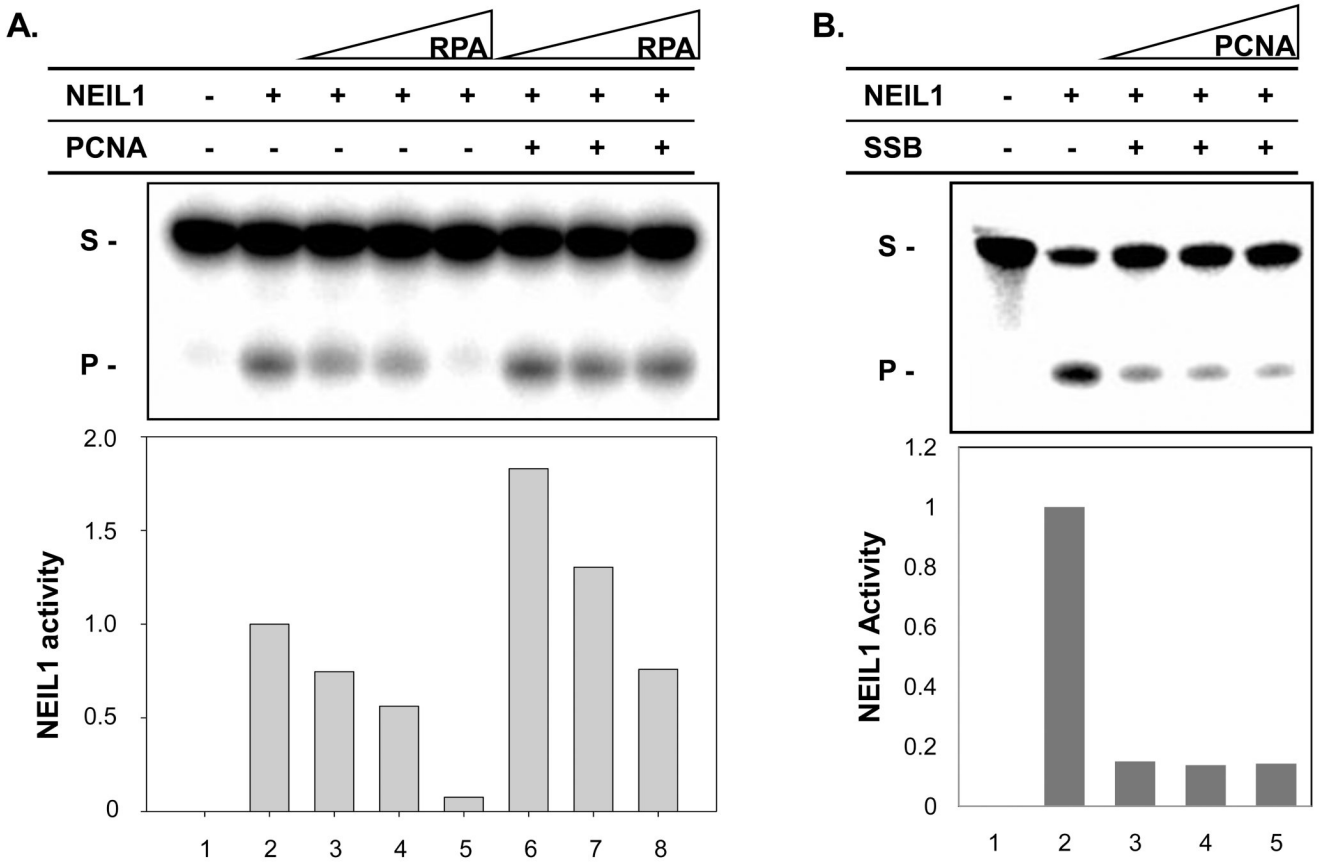

Figure 9. PCNA relieves NEIL1 inhibition by RPA

A. NEIL1 activity on 5-OHU-containing Rep 21 substrate (25 nM) with no enzyme (lane 1), NEIL1 alone (1 nM; lane 2), in the presence of increasing RPA:DNA molar ratio (1.25:1, 2.5:1 or 5:1; lanes 3–5) or in the presence of increasing RPA with PCNA (2 μM; lanes 6–8). **B.** NEIL1 activity alone (lane 2) or in the presence of 2.5:1 molar ratio of SSB to DNA substrate with increasing concentration of PCNA (lanes 3–5). DNA was pre-incubated with RPA or SSB at 4°C for 30 min prior to addition of other proteins.

Table 1

Structures of DNA substrates used in the present study. (X represents 5-OHU)

ssDNA
3'-CCG TGC CAG ATG TGC CGT GTG CTC AXA TGT ACT ATG CTA AGG TTC GAT TCG - 5'
Rep 15
5' - GGC ACG GTC TAC ACG - 3'
3' - CCG TGC CAG ATG TGC CGT GTG CTC AXA TGT ACT ATG CTA AGG TTC GAT TCG - 5'
Rep 21
5' - GGC ACG GTC TAC ACG GCA CAC - 3'
3' - CCG TGC CAG ATG TGC CGT GTG CTC AXA TGT ACT ATG CTA AGG TTC GAT TCG - 5'
Rep 24
5' - GGC ACG GTC TAC ACG GCA CAC GAG- 3'
3' - CCG TGC CAG ATG TGC CGT GTG CTC AXA TGT ACT ATG CTA AGG TTC GAT TCG - 5'
Rep 29
5' - GGC ACG GTC TAC ACG GCA CAC GAG TGT AC- 3'
3' - CCG TGC CAG ATG TGC CGT GTG CTC AXA TGT ACT ATG CTA AGG TTC GAT TCG - 5'
dsDNA
3' - CCG TGC CAG ATG TGC CGT GTG CTC AXA TGT ACT ATG CTA AGG TTC GAT TCG - 5'
5' - GGC ACG GTC TAC ACG GCA CAC GAG TGT ACA TGA TAC GAT TCC AAG CTA AGC - 3'